Structural Eng. / Earthquake Eng. Vol. 6. No. 2, 283s-294s. October 1989
Japan Society of Civil Engineers (Proc. of JSCE No. 410/I-12)

FRACTURE ANALYSES OF CONCRETE STRUCTURES BY THE MODIFIED DISTINCT ELEMENT METHOD

By Kimiro MEGURO and Motohiko HAKUNO***

A new method for analyzing the fracture of concrete structures is proposed in which concrete is considered a granular assembly. Because concrete is a complex, extremely heterogeneous material, it is difficult to analyze it's failure properties by the Finite Element Method (FEM) in which concrete is considered a homogeneous, continuous medium. We have developed a Modified Distinct Element Method (MDEM) that can be applied to the problems of fracture of concrete structures. In the MDEM the respective major constituents of concrete, gravel and mortar, are represented as circular particle elements and nonlinear springs, called pore-springs. We have used the MDEM to simulate the dynamic fracture behavior of concrete structures. The numerical results obtained are in good agreement with the seismic damage recorded during past earthquakes.

Keywords : distinct element method, modified distinct element method, concrete structure, discontinuous material analysis, fracture analysis

1. INTRODUCTION

Various fracture analyses of concrete structures have been made by the Finite Element Method (FEM) in which concrete has been considered a homogeneous, continuous medium. The FEM, however, is suitable only for studying the processes that take place up to fracture. Concrete is a complex, extremely heterogeneous material, whose fracture strength and mode depend on the strength, size, quantity, and distribution of the gravel as well as the quality of the mortar used. Therefore the fracture properties of concrete can not be analyzed by the FEM, and establishing a method of analysis by which its fracture properties can be analyzed is a major goal of concrete fracture mechanics. We here propose a new method for the analysis of the fracture of concrete structures, in which concrete is considered a granular assembly.

We have extended Cundall's Distinct Element Method (DEM), a method used to analyze discontinuous material, to the problems of the fracture of concrete structures. The conventional DEM, however, can not be applied to a concrete medium because the effects of the mortar and surrounding gravel can not be accounted for by this method. We have developed a Modified Distinct Element Method (MDEM), which can be used with a complex or heterogeneous material such as concrete, and have applied it to the problems of fracture of concrete structures which can not be solved by the conventional DEM. In our MDEM, the respective major constituents of concrete, gravel and mortar, are represented as circular particle elements and nonlinear springs, which we have called pore-springs. This MDEM method can follow the total fracture process even after the medium becomes discontinuous. Nonlinear phenomena such as the shear band and the effects of dilatancy are simulated

* Member of JSCE, M. Eng., Graduate Student, Department of Civil Engineering, University of Tokyo. (Yayoi 1-1-1 Bunkyo-ku, Tokyo 113, JAPAN)
** Member of JSCE, Dr. Eng., Professor, Earthquake Research Institute, University of Tokyo. (Yayoi 1-1-1 Bunkyo-ku, Tokyo 113, JAPAN)

automatically. Both the overall mode of fracture and the microscopic fracture mechanism that operates between gravels can be obtained, and the heterogeneity of the material can be considered as the dispersion of the particle elements. We have used this MDEM method to simulate the dynamic fracture behavior of concrete structures. The numerical results obtained agree well with laboratory results as well as with the actual seismic damage reported during past earthquakes.

Optimum use of the MDEM requires many calculations that require sophisticated electronic computers. Fortunately, the calculation speed and memory capacity of electronic computers have been improving markedly year by year, and the future optimum use of the MDEM is feasible. We therefore believe that the MDEM will prove a useful method by which to analyze the fracture of concrete structures.

2. Modified Distinct Element Method (MDEM)

The conventional DEM has been used in geotechnical engineering and has proved very useful[3),4)]. So far, however, there has been no report of the DEM being applied to other media. We have expanded the use of the DEM by applying it to the analysis of the fracture of concrete structures which have been analyzed only by continuous material methods such as the FEM. We developed a new Distinct Element Method program, which can be used not only for geotechnical engineering, but with other media and which incorporates a modified Iwashita's model[6)]. We have named it the Modified Distinct Element Method (MDEM). This model has continuity because of the introduction of the pore material spring. Fig. 1 shows the modeling of concrete for the MDEM model.

The use of the DEM has been widely expanded by the MDEM simulation program. The MDEM model gradually becomes plastic as the pore-springs are destroyed. The MDEM expresses the nonlinearity of the medium, automatically; while the pore-springs are in tact, the model behaves as a continuous medium; but, as the pore-springs are destroyed, it gradually loses continuity, finally behaving as a perfect discrete body (Fig. 2). This phenomenon is very similar to that in which by heating, matter changes from a solid to a liquid and/or gas, with gradual loss of continuity between its molecules. With the MDEM, a series of analyses (from continuous to discontinuous) can be made, and the method can be easily applied to both discontinuous and nonlinear phenomena so that every element separates and moves widely after the destruction of the pore-springs, a new stress field being formed by contacts between elements which were not previously in contact. One particularly good point of the MDEM is that as its pore-springs are destroyed, the structure of the model changes gradually from elastic to plastic so that nonlinear phenomena (e. g., the shear band and effects of dilatancy) can be simulated automatically. Fig. 3 outlines the MDEM simulation flow.

(1) Division of the model and the array of material parameters

The simplest way to apply the conventional DEM to complex material is for every element to have different parameters; but, this requires a large memory capacity, especially when a large granular assembly is used. Therefore we divided the model into several parts that correspond to the actual objective medium, and assigned material parameters to each part. Of the two ways to divide the model—by element number or by element coordinate—we have used element coordinates because of their easier application to a random packed model. After establishing the element type (NTP) of each division, we then assigned the material parameters of the NTP.

(2) Equation of motion

The motion of a particle element, i, having the mass, m_i, and the moment of inertia, I_i, is

$$m_i\ddot{\boldsymbol{u}}+C_i\dot{\boldsymbol{u}}+F_i=0 \quad \cdots\cdots (1)$$

$$I_i\ddot{\phi}+D_i\dot{\phi}+M_i=0 \quad \cdots\cdots (2)$$

in which F_i is the sum of all the forces acting on the particle; M_i the sum of all the moments acting on it; C_i and D_i the damping coefficients; $\boldsymbol{u}$ the displacement vector; and ϕ the angular displacement.

The time history of $\boldsymbol{u}$ and ϕ can be obtained step-by-step in the time domain by the numerical integration of these equations.

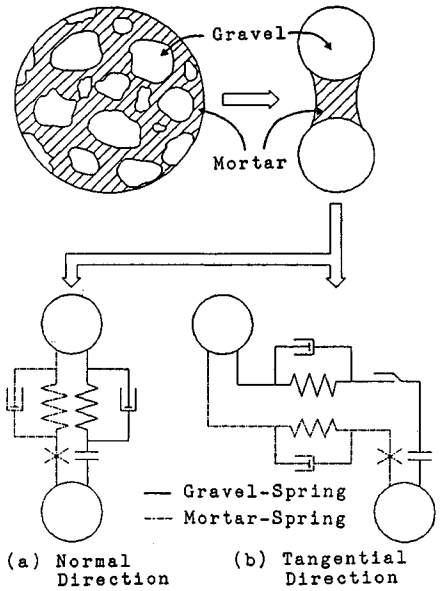

Fig. 1 Modeling of Concrete for MDEM.

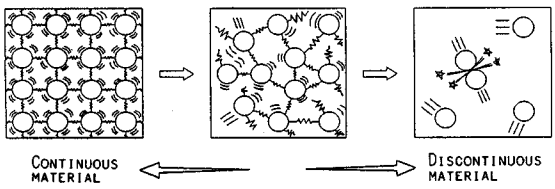

Fig. 2 Behavior of the MDEM Model.

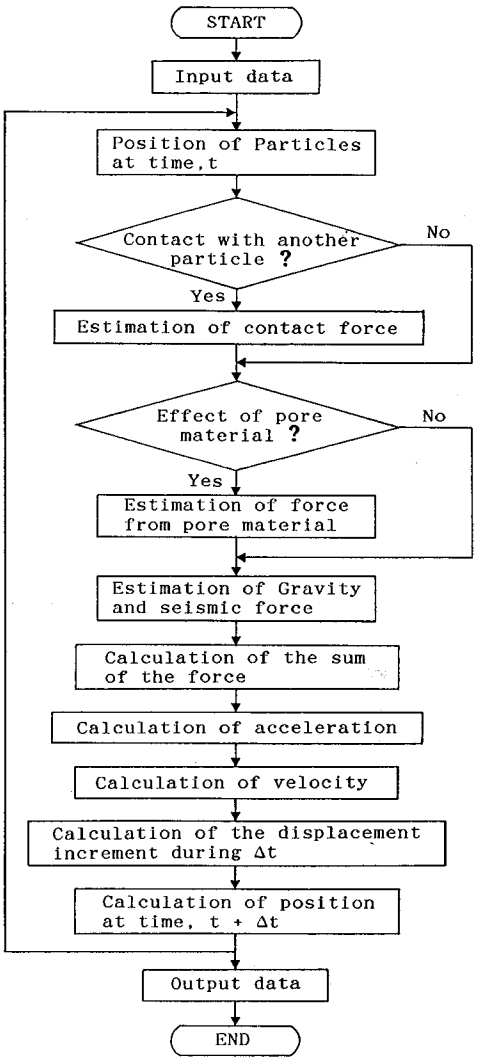

Fig. 3 Flow of MDEM Simulation.

(3) Establishment of the pore-spring and fracture criteria

a) Establishment of the pore-spring

To account for the pore material in the MDEM model, we introduced additional mortar springs (pore-springs) between elements in both the normal and tangential directions (Fig. 1). The establishment of the pore-spring is shown among the pores between elements, i and j (element type, NTP (i)=NTP (j)=n 1) which belong to division n 1. The pore-spring is established when the distance between these two elements satisfies eq. (3).

When the respective coordinates of element i (radius, r_i) and j (radius, r_j) are (X_{i0}, Z_{i0}) and (X_{j0}, Z_{j0}) at time zero, the critical equations for pore-spring establishment are

$$(r_i+r_j)\times\alpha(n\,1)>[D_{ij}]_0 \quad \cdots\cdots (3)$$

in which

$$[D_{ij}]_0=\sqrt{(X_{i0}-X_{j0})^2+(Z_{i0}-Z_{j0})^2} \quad \cdots\cdots (4)$$

and α (n 1) is the critical value for pore-spring establishment.

The natural length of the pore-spring ($=L_{ij}$) is memorized as the initial distance between elements i and j according to

$$L_{ij}=[D_{ij}]_0 \quad \cdots\cdots (5)$$

b) Fracture criteria for the pore-spring

At first, the pore material between particles is firmly and stably associated with them. But when an external force acts on the model, the elements begin to move, and cracks are produced in the pore material by tensile or shear force. Because of these cracks, the pore material will have lost its tensile resistance and will resist compressive and shear deformation only while compressive force acts between the particles. On the basis of these phenomena, we have divided the fracture process of the pore-spring into 2 states :

State 1 : The pore-spring is normal. It resists not only compression but tension and shearing deformation when external compressive or tensile forces act on it.

State 2 : Cracks are produced in the pore material. The effect of the pore-spring is viable only while compressive force acts between the elements. The pore-spring has no tensile resistance. It resists compressive and shearing deformation only while compressive force acts between the elements.

The two conditions under which the pore-spring situation changes from the 1 st to the 2 nd state are

1) When the pore-spring is fractured by tensile force in the normal direction.

2) When the pore-spring is fractured by shear force in the tangential direction.

During MDEM calculations, the cause of each crack in the pore-spring is memorized. When all the pore-springs were established, each was in the 1 st state ; but the state changes by the following fracture criteria :

1. Fracture criteria in the normal direction

The critical strain on the pore-spring is specified in the normal direction. The pore-spring changes from the 1 st to the 2 nd state when the strain on it at time t satisfies eq. (6). $\beta\ (n\ 1)$ is the critical strain on division n 1.

$$[D_{ij}]_t > \beta\,(n\,1) \times L_{ij} \quad \cdots\cdots (6)$$

in which $[D_{ij}]_t$ is the distance between the two centers of elements i and j at time t, and L_{ij} is the initial length of the pore-spring between these two elements.

Although these criteria show that pore-spring cracking is produced by tensile strain in the normal direction, pore-springs in both the normal and tangential directions are assumed to change from the 1 st to the 2 nd state. At the same time, the cause of pore-spring destruction is memorized as tensile strain in the normal direction.

2. Fracture criteria in the tangential direction

Coulomb's equation gives the fracture criteria for the pore-spring in the tangential direction, and is expressed as

$$\tau_c = C + \mu \times F_n \quad \cdots\cdots (7)$$

in which τ_c is the maximum, resistant shear force between particles in the tangential direction ; C is the cohesive constant force ; μ the friction coefficient ; and F_n the normal force acting between particles i and j.

When the force acting tangentially on the pore-spring is larger than τ_c in eq. (7), the state of the pore-spring in both the normal and tangential directions is assumed to change to state 2. At that time, the cause of fracture is memorized as the shearing force, and the force acting tangentially on this pore-spring becomes τ_c.

(4) All the forces that act on a particle

In MDEM analysis, two kinds of forces act on a particle ; the force received from all the particles in contact and the force of all the pore material surrounding the particle. These forces are obtained from the deformation of the element and the pore material springs set in the normal and tangential directions.

At time t, the x and z direction components of all the forces acting on element, i, $[Fx_i]_t$ and $[Fz_i]_t$ and all the moments acting on it, $[M_i]_t$ are

$$[Fx_i]_t = [Fx_{ie}]_t + [Fx_{ip}]_t + m_i \times a_x \quad \cdots\cdots (8)$$

$$[Fz_i]_t = [Fz_{ie}]_t + [Fz_{ip}]_t - m_i \times g + m_i \times a_z \quad \cdots\cdots (9)$$

$$[M_i]_t = [M_{ie}]_t + [M_{ip}]_t \quad \cdots\cdots (10)$$

in which $[Fx_{ie}]_t$ and $[Fz_{ie}]_t$ are x and z direction components of all the forces acting on element i by all the

elements in contact, $[Fx_{ip}]_t$ and $[Fz_{ip}]_t$ are the x and z direction components of all the forces of all the surrounding pore material that act on the element. $[M_{ie}]_t$ is the sum of all the moments of all the elements in contact, and $[M_{ip}]_t$ of all the pore material surrounding the element. In eq. (9), g is the acceleration of gravity, and shows that gravity acts in the $-z$ direction.

We expressed an external force which acts on the model in one of two ways, that force being the input at the supporting elements (as in earthquake loading), or the force given by the direct action of acceleration on every element of the model. The values of a_x and a_z in eqs. (8) and (9) are the accelerations in the x and z directions for the latter expression of external force. To simplify the MDEM, we used the model shown in Fig. 1, but a more complex model could easily have been used.

3. ESTIMATION OF THE MATERIAL PARAMETERS OF THE MDEM

Although the material parameters of MDEM analysis should be determined experimentally, it is impossible to do so in certain cases. Therefore, we have proposed a simple method by which to determine these parameters, which takes into account the physical significance of each parameter. The details of this method are given in reference 2).

a) Estimation of the elastic constants of the element spring and the pore-spring

The spring constants of the elements and pore material springs can be determined from the wave velocity in the objective medium. The propagation velocities of the P and S waves are obtained by use of Young's modulus, Poisson's ratio and the density. We assume that the elastic constant of the normal spring is estimated by V_p and that of the tangential is estimated by V_s. The composite elastic constant of an element and the pore material spring are obtained in both directions. From these composite values, the elastic constants of the element and pore material in both directions can be calculated.

b) Estimation of the time increment, Δt

The MDEM is based on numerical integration. The stability of the analysis depends on the value of the time increment, Δt. It is necessary to determine the proper value of Δt. We determined this time increment, (Δt) as follows : In the MDEM, the forces that act on each element are calculated taking into account all the contacting elements and the pore material surrounding an element. Reactional forces can not be estimated well if the stress wave goes over the contacting element during the time increment, Δt. Therefore, a rough determination Δt is

$$\Delta t < D_{\min}/V \quad \cdots\cdots (11)$$

in which V is the wave propagation velocity, and $D_{\min}$ the minimum distance between the centers of two elements.

4. NUMERICAL RESULTS

(1) Fracture test of a concrete specimen

We used the MDEM to make a numerical simulation of a one-axis compression fracture test of the concrete specimen modelled in Fig. 4. The specimen was compressed vertically under constant-rate deformation during each time step. The fracture process during compression is shown. The top row in Fig. 4 shows the particle distribution; the position of the gravel. The middle row shows the pore-spring (mortar-spring) distribution; the position of undestroyed mortar. The bottom row shows the velocity distribution.

During stage 1, no cracks occur in the particle or spring locations. Should a crack occur, the pore-spring at the corresponding site would disappear; therefore, development of a crack and its position can be determined from the pore-spring location. Stage 2 shows the incidence of diagonal shear cracks in the specimen. Careful observation of the shear cracking planes shows that they are formed by many small cracks produced continuously along a particular plane by the tensile force. These small cracks occur parallel to the loading direction because the pore-springs in the horizontal direction disappear. Although the cracks in stage 2 are called shear cracks, most are produced by tension. The fracture, called shear cracking, is considered to be

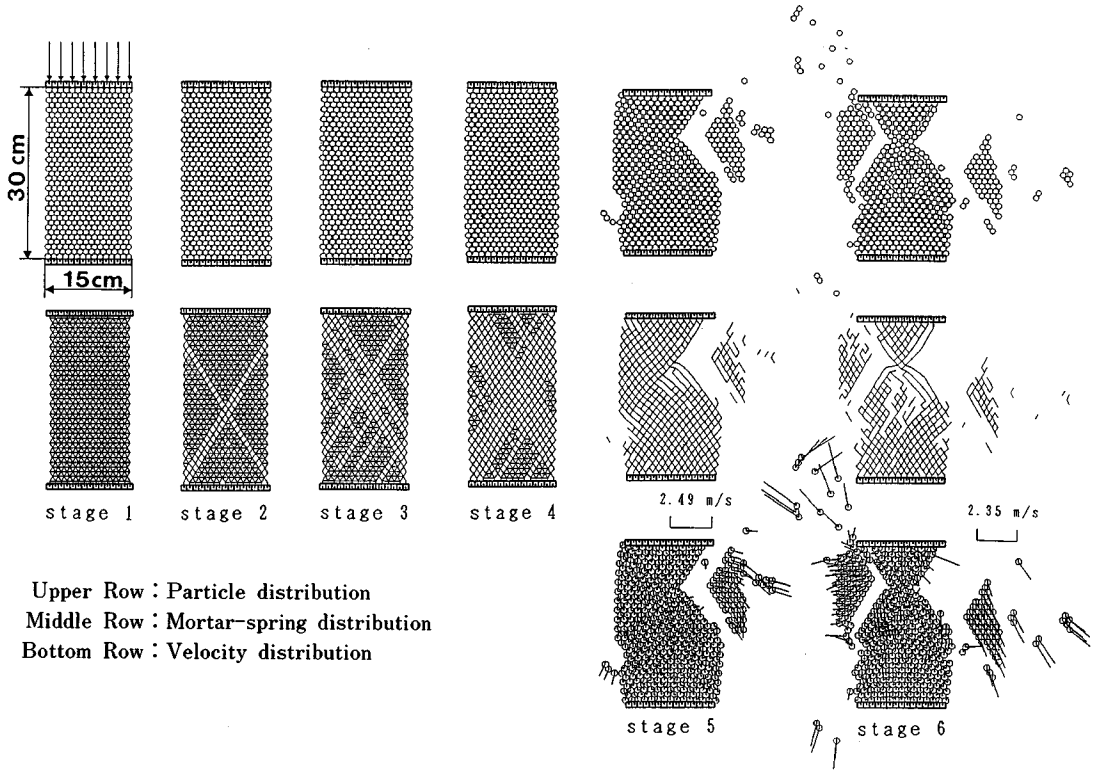

Fig. 4 Fracture Process during a Compression Test on a Concrete Specimen under Vertical, Constant-rate Deformation.

formed by many microscopic cracks produced by the tensile force along a particular plane.

As the stage progresses, fracture gradually extends in the direction parallel to the past fracture. In stages 5 and 6 a slab of destroyed concrete separates and is sloughed off from the main body of the specimen. The separation of the concrete slab cannot be analyzed by traditional methods such as the FEM. The numerical results produced by the MDEM agree with the results of past laboratory tests.

(2) Impulsive fracture analysis of a rigid-frame, masonry concrete structure

We used the model shown in Fig. 5, to analyze the fracture behavior of a rigid-frame, masonry concrete structure that was subjected to a horizontal impulsive force. The diagram at left in the upper row of the figure shows particle distribution in the initial state. The other diagrams in this row show the normal compressive force distributions. The diagrams in the bottom row show the mortar-spring distributions.

In stage 2, shear cracks appear at the foot of the frame. During this stage, the normal force distribution shows concentrated stress at the foot of the frame. In stage 3, the fracture at the foot of the frame has advanced, and the frame has separated completely from the supporting ground elements. During this stage there is no concentrated stress at the foot of the fame where there had been large stress in stage 2. In stage 3, concentrated stress acts on the beam-column connections, causing concentrated fractures at those connections in stages 3 and 4. Photos 1 and 2 show damage done in the Off-Miyagi Prefecture earthquake (1978) and the Mexico earthquake (1985). Cracks produced by concentrated stress are clearly shown at the corners of the frame.

(3) Dynamic fracture analysis of a masonry concrete structure

We used the three models shown in Figs. 6 to 8 to analyze the dynamic fracture of a masonry concrete wall subjected to sinusoidal, horizontal force. Model 1 (Fig. 6) consists of an arrangement in which the centers of

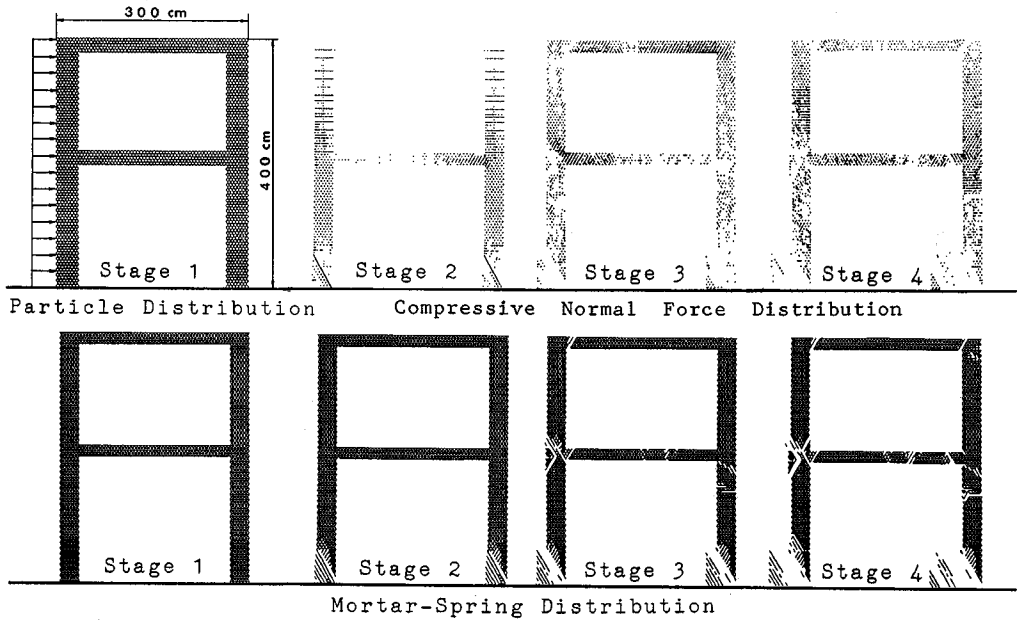

Fig. 5 Fracture Process of a Rigid-Frame, Concrete Structure under Horizontal Impulsive Loading.

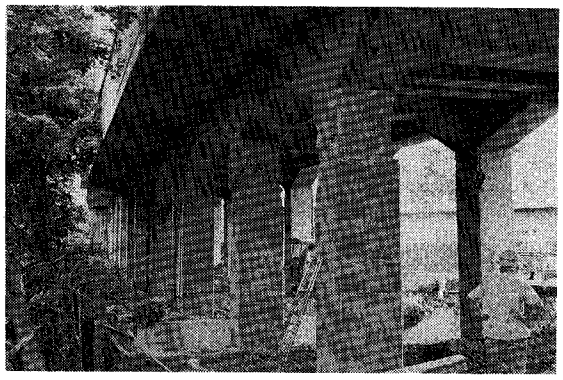

Photo 1 Cracks in a Concrete Frame (Off-Miyagi Prefecture Earthquake 1978).

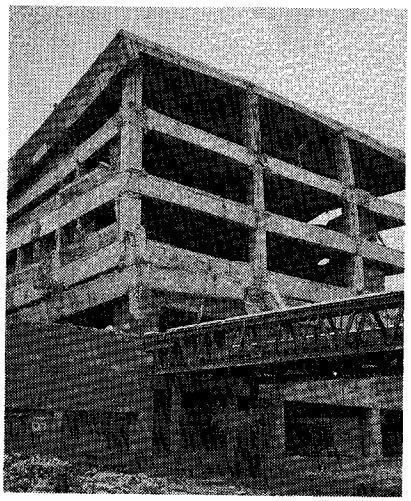

Photo 2 Cracks in a Concrete Frame (Mexico Earthquake 1985).

the elements are equilateral triangles. Model 2 (Fig. 7) is a random-packing model. Model 3 (Fig. 8) has the same element arrangement as model 1, but the wall is surrounded by a strong concrete frame. No special joint effects between walls and columns (such as reinforcement) have been considered.

The dynamic fracture of model 1 is shown in Fig. 6. First shear cracks were produced, then when force was applied in the reverse direction, new cracks that crossed the original ones formed. A comparison of Fig. 6 (a) with (b) shows that these cracks extend in the direction in which the large compressive force acts and that each microscopic crack is produced by the tensile effect. The directions of all the small cracks are parallel to the compressive loading direction. When the external force is vibratory, crossing shear cracks are produced because the direction of loading changes. This pattern of crossing shear cracks caused by vibrational external force has been found frequently in walls after past earthquakes (Photo 3). At the boundary between the

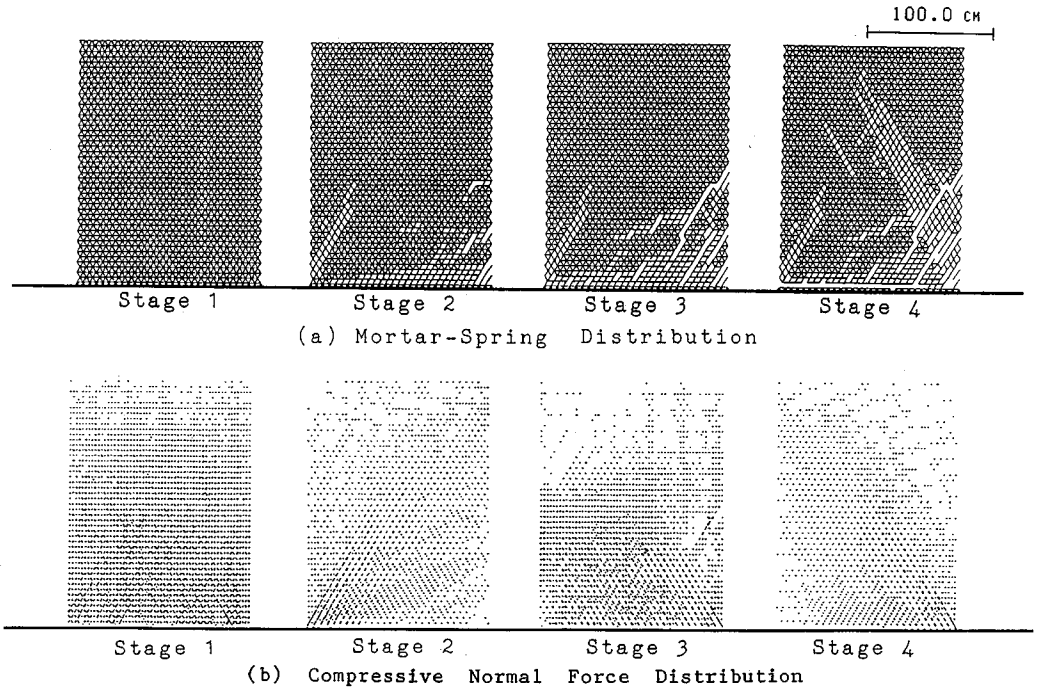

Fig. 6 Fracture Process of a Masonry Concrete Wall under Sinusoidal, Horizontal Loading (Model 1).

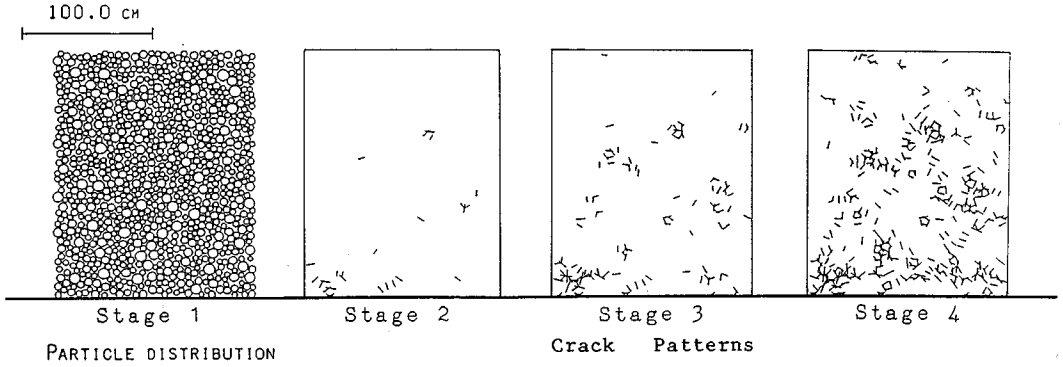

Fig. 7-1 Fracture Process of a Masonry Concrete Wall under Sinusoidal, Horizontal Loading (Model 2).

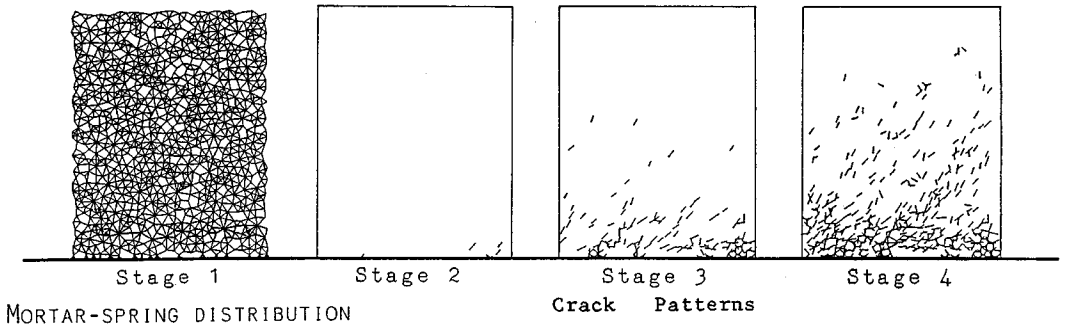

Fig. 7-2 Fracture Process of a Masonry Concrete Wall under Sinusoidal, Horizontal Loading during the 1/2 period (Model 2).

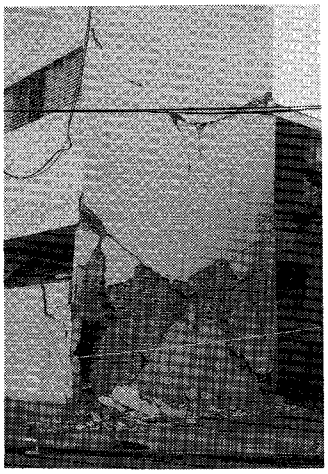

Photo 3 Typical Shear Cracks in a Brick Wall (Mexico Earthquake 1985).

Photo 4 No Connecting Steel Bar between the Column and Wall (Equador Earthquake 1987).

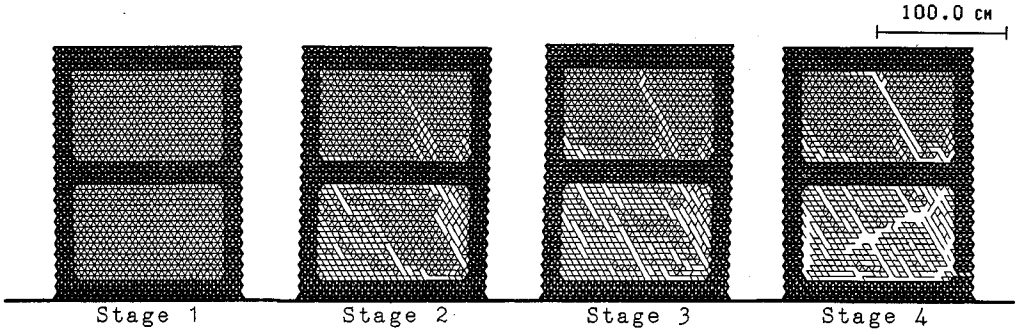

Fig. 8 Fracture Process of a Masonry Concrete Wall with a Frame under Sinusoidal, Horizontal Loading (Model 3, Mortar-spring Distribution).

structure and the ground, where there is concentrated stress, large cracks are produced. These phenomena also can be simulated with models 2 (Fig. 7-1, 7-2) and 3 (Fig. 8). Fig. 7-2 shows the fracture process under horizontal, sinusoidal loading during the 1/2 period, the relation between the loading direction and crack pattern is clear.

The process of fracture for model 3 is shown in Fig. 8. Because of the effect of the strong concrete frame that surrounds the wall, fracture occurs within the wall, particularly at the bottom. During stage 4, large cracks appear at the boundary between the column and the bottom wall. These seem to form because there is no effective joint at this boundary. Actual earthquake damage also shows large cracks between a column and wall (Photo 4) where no joint (such as a reinforcement) was present. When the external vibrational force is very strong, fracture sometimes occurs in the frame as well (Photo 5). In our analysis, in addition to the shear cracks seen in the bottom wall, the bottom of the right frame column also has been destroyed. This type of fracture seems to be the same phenomenon as that seen in Photo 5.

(4) Dynamic fracture analysis of a reinforced concrete (RC) structure

We analyzed the dynamic fracture behavior of RC structures subjected to sinusoidal, horizontal force (amplitude, 980 gal period, 0.2 s) with two models (Fig. 9 [model 1] and Fig. 10 [model 2]). We used model 2 to investigate the mode fracture based on differences in the length of reinforcements when the reinforcing steel bars reach only to half the height of the model. Young's modulus for a steel bar, which

is 15-fold that of concrete, was used.

Fracture in an RC structure with long reinforcement bars is shown in Fig. 9. The mortar-spring distribution is given in Fig. 9 (a) and the normal compressive force between elements in Fig. 9 (b). The bolt lines in Fig. 9 (a) show the reinforcing steel bars. A comparison of Figs. 9 (a) and (b) shows that cracks are produced in the direction in which the external force acts. During stage 2 in Fig. 9 (a), noncontinuous cracks have jumped the concrete near the steel bar because of the reinforcing effect. But, because of the difference in Young's modulus for steel and concrete, the external forces clearly are concentrated at the steel bars and the nearby concrete, resulting in the many cracks in the mortar adjacent to the reinforcing bars. Crossing shear cracks also occur in the concrete between the steel bars.

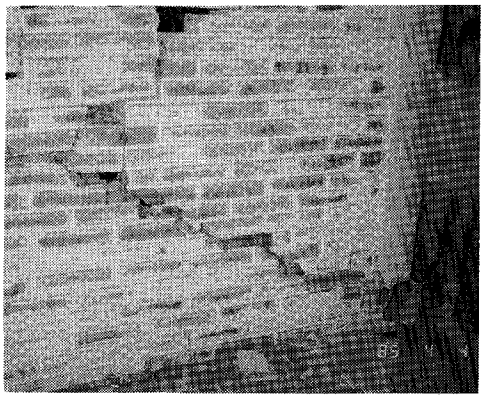

Photo 5 Fracture of a Brick Wall with a Frame (Chile Earthquake 1985).

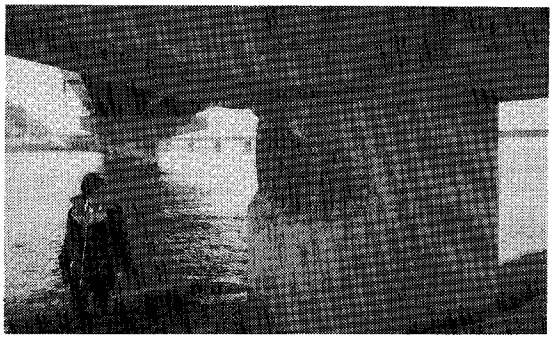

Photo 6 Fracture of an RC Structure at the point of Discontinuous Reinforcement (Off-Urakawa Earthquake 1982).

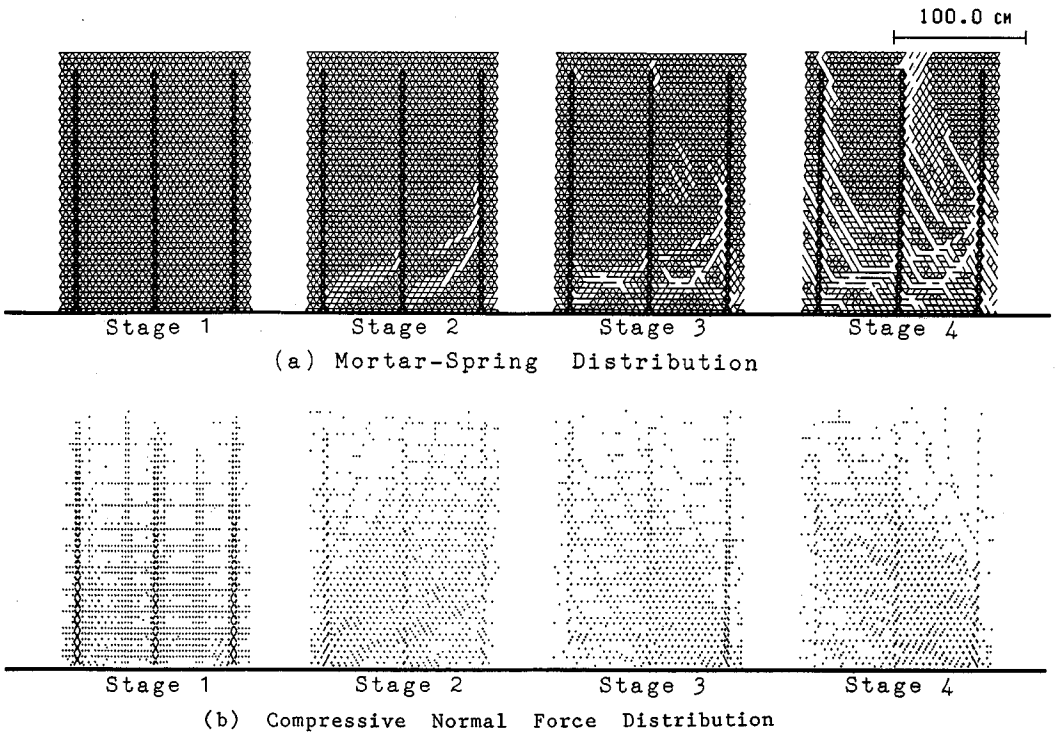

Fig. 9 Fracture Process of an RC Structure under Sinusoidal, Horizontal Loading (Model 1).

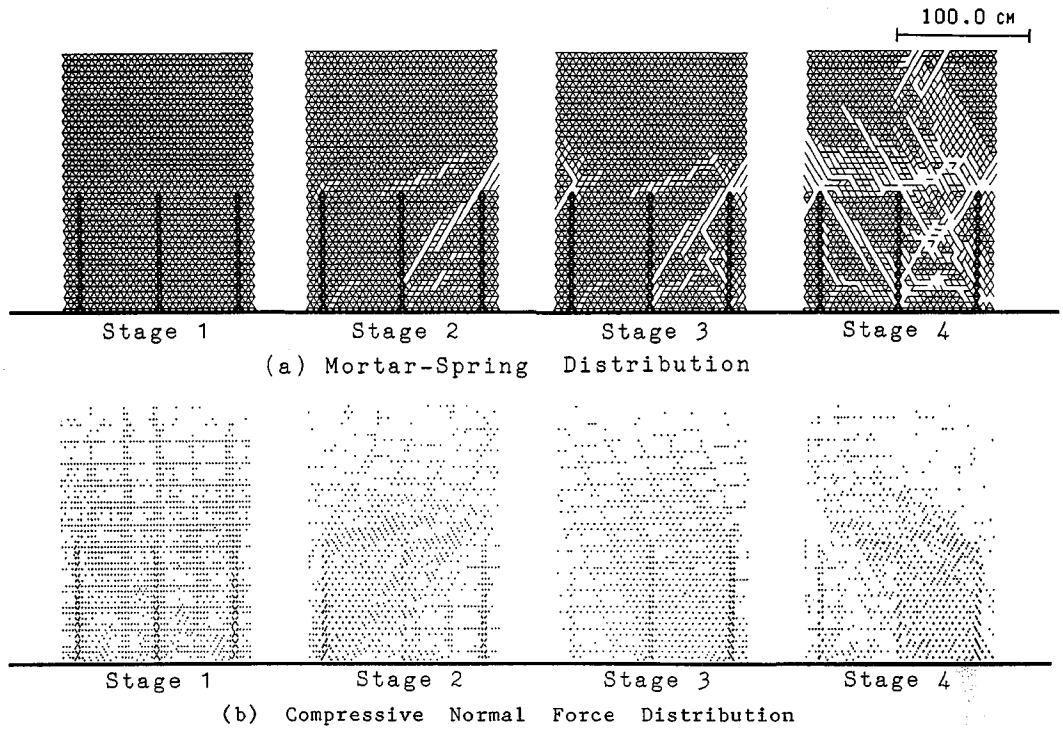

Fig. 10 Fracture Process of an RC Structure Reinforced with Short Steel Bars under Sinusoidal, Horizontal Loading (Model 2).

The fracture process with model 2, an RC structure reinforced with short steel bars, is shown in Fig. 10. Cracks appear in the direction in which the external force acts, as in the other analyses; but, an additional horizontal crack is present approximately at the top of the reinforcing bars. This phenomenon also has been found after earthquake damage (Photo 6), in the Off-Urakawa earthquake of 1982. Horizontal cracks are present at mid height of the pier, where reinforcement ends and the steel ratio changes. Our numerical results are in good agreement with the observed phenomenon.

5. CONCLUSIONS

We have here proposed use of the Modified Distinct Element Method (MDEM) as a new method for analyzing the fracture of concrete structures. The MDEM is a discrete material analysis method that we established on the basis of Iwashita's model in order to extend the use of the Distinct Element Method (DEM). In the MDEM, the gravel present in the concrete was idealized as circular particle elements and the mortar as nonlinear springs (called pore-springs).

It enables us to analyze a series of behavior, of a complex, heterogeneous material that changes from a continuous to a discrete medium. As its pore-springs are destroyed, the structure of the MDEM model gradually changes from an elastic to a plastic material. Also, nonlinearities such as the shear band and effects of dilatancy are simulated automatically. We applied the MDEM to a test of the fracture of a concrete specimen and to dynamic analyses of fractured concrete structures.

The numerical results obtained are in good agreement with those of past laboratory tests as well as with actual seismic damage observed after past earthquakes. They confirm that the MDEM is an effective method for the analysis of the fracture of concrete structures.

ACKNOWLEDGMENTS : We are very grateful to Dr. Hazime Okamura (Professor, the University of

Tokyo) for his many helpful suggestions.

REFERENCES

1) Cundall, P. A. : A Computer Model for Simulating Progressive, Large Scale Movement in a Blocky Rock System, Symp. ISRM, Nancy, France, Proc., Vol. 2, pp. 129-136, 1971.
2) Meguro, K. and Hakuno, M. : Fracture Analyses of Concrete Structures by Granular Assembly Simulation, Bulletin of The Earthquake Research Institute, University of Tokyo, Vol. 63, Part 4, pp. 409-468, 1988 (Japanese with English abstract).
3) Kiyama, H. and Fujimura, H. : The Analysis of the Gravity Flow of Granular Rock Assemblies using Cundall's Model, Proc. of Japan Society of Civil Engineers, No. 333, pp. 137-146, 1983 (in Japanese).
4) Uemura, D. and Hakuno, M. : A Granular Assembly Simulation with Cundall's Model for the Dynamic Collapse of a Structural Foundation, Structural Eng./Earthquake Eng. Vol. 4, No. 1, pp. 181-190 (Proc. of JSCE No. 380), Japan Society of Civil Engineers, 1987.
5) Hakuno, M. and Tarumi, Y. : A Granular Assembly Simulation for the Seismic Liquefaction of Sand, Structural Eng./Earthquake Eng. Vol. 5, No. 2, pp. 129-138 (Proc. of JSCE No. 398), Japan Society of Civil Engineers, 1988.
6) Iwashita, K. and Hakuno, M. : Granular Assembly Simulation for Dynamic Cliff Collapse due to Earthquake, Proc. of 9 WCEE, Vol. 3, pp. 175-180, 1988.

(Received October 31 1988)